Atmos. Chem. Phys. Discuss., 14, 1349–1374, 2014
www.atmos-chem-phys-discuss.net/14/1349/2014/
doi:10.5194/acpd-14-1349-2014

Atmospheric Chemistry and Physics Discussions
Open Access

Where do the air masses between double tropopauses come from?

A. C. Parracho, C. A. F. Marques, and J. M. Castanheira

CESAM, Department of Physics, University of Aveiro, Portugal

Received: 19 December 2013 – Accepted: 3 January 2014 – Published: 17 January 2014

Correspondence to: J. M. Castanheira (jcast@ua.pt)

Published by Copernicus Publications on behalf of the European Geosciences Union.

Abstract

An analysis of the origin of air masses that end up between double tropopauses (DT) in the subtropics and midlatitudes is presented. The double tropopauses were diagnosed in the ERA-Interim reanalysis (1979–2010), and the origin of air masses was analysed using the Lagrangian model FLEXPART.

Different processes for the formation of double tropopauses (DT) have been suggested in the literature. Some studies have suggested that double tropopauses may occur as a response to the vertical profile of adiabatic heating, due to the residual meridional circulation, while others have put forward contradicting explanations. Whereas some studies have suggested that double tropopauses result from poleward excursions of the tropical tropopause over the extratropical one, others have argued that DTs develop in baroclinic unstable processes involving transport of air from high latitudes.

In some regions, the DT structure has a semipermanent character which cannot be explained by excursions of the tropical tropopause alone. However, the results presented in this paper confirm that processes involving excursions of the tropical tropopause over the extratropical tropopause, which are therefore accompanied by intrusions of air from the tropical troposphere into the lower extratropical stratosphere, make a significant contribution for the occurrence of DTs in the subtropics and midlatitudes. Specifically, it is shown that the air between double tropopauses comes from equatorward regions, and has a higher percentage of tropospheric particles and a lower mean potential vorticity.

1 Introduction

In the last 10–15 yr, several studies have focused on tropopause dynamics (see Fueglistaler et al., 2009, and Gettelman et al., 2011 for a review). In those studies two tropopause features have received special attention. One of these features, first

ACPD

14, 1349–1374, 2014

Title Page
Abstract Introduction
Conclusions References
Tables Figures
◂ ▸
Back Close
Full Screen / Esc
Printer-friendly Version
Interactive Discussion

reported by Birner (2002), consists of a strong increase of temperature with height in a layer just above the tropopause. This layer is now called the Tropopause Inversion Layer (TIL). The temperature increase in the TIL is associated with a distinct maximum in static stability parameter N^2, above which N^2 decays roughly exponentially toward typical stratospheric values (Birner, 2006). Another feature is the occurrence of double tropopause (DT) layers, i.e. layers between two levels whose thermal lapse rates satisfy the WMO (1957) definition of thermal tropopause. Double tropopauses are frequent events in the subtropics and midlatitudes (Añel et al., 2008; Castanheira and Gimeno, 2011).

The physics and dynamics that control these two features are not completely understood yet. For example, Randel et al. (2007a) and Kunz et al. (2009) suggested a radiative forcing mechanism for the TIL, whereas Birner (2010a), based on model experiments, showed that the dynamical warming due to residual stratospheric circulation is the main driver of the TIL at midlatitudes. Different explanations for the occurrence of DTs have also been suggested. Randel et al. (2007b) and Pan et al. (2009) presented observational evidence that double tropopause structures could result from excursions of the tropical tropopause over the extratropical tropopause, accompanied by intrusions of tropical air from the troposphere into the lower extratropical stratosphere. The results of Castanheira and Gimeno (2011) and Castanheira et al. (2012) are consistent with that mechanism. However, Wang and Polvani (2011) and Añel et al. (2012) argued that the air particles found between double tropopauses come from high latitudes, not from the tropics/subtropics. Moreover, Birner (2010a) suggests that double tropopauses in subtropics may result from a dipolar forcing (positive just above the extratropical tropopause and negative below the tropical tropopause) of the static stability by the residual circulation, a forcing also associated with the formation of the TIL.

This study is an attempt to bring out additional knowledge about the occurrence of DTs, by presenting a systematic analysis of the origin of air particles that end up between double tropopauses diagnosed in the ERA Interim reanalysis. We analyse the backward trajectories of the particles, the potential vorticity field (PV), and the fraction

ACPD
14, 1349–1374, 2014

of tropospheric particles found between DTs. Our results show that air masses found between double tropopauses come from regions which are equatorward (smaller latitudes and smaller PV values) of the regions from where the air masses associated with single tropopauses (STs) are found to come; and that DTs are frequently associated with tropospheric intrusions into the lower extratropical stratosphere.

Section 2 describes the data, the Lagrangian model, and the analysis method used. The main results are given in Sect. 3, and Sect. 4 closes the paper with some concluding remarks.

2 Data, backward trajectories, and analysis method

2.1 Double tropopause dataset

The first and, if present, second thermal lapse rate tropopauses were identified using the conventional WMO (1957) criteria:

a. The *first tropopause* is defined as the lowest level at which the lapse rate decreases to $2\,\mathrm{K\,km^{-1}}$ or less, provided that the average lapse rate between this level and all higher levels within 2 km does not exceed $2\,\mathrm{K\,km^{-1}}$.

b. If above the first tropopause the average lapse rate between any level and all higher levels within 1 km exceeds $3\,\mathrm{K\,km^{-1}}$ then a *second tropopause* is defined by the same criterion as in a. This tropopause may be either within or above the 1 km layer.

These criteria were applied to the ERA Interim reanalysis (Dee et al., 2011) on isobaric levels using an algorithm that is similar to that used by Birner (2010b) (which in turn is a slight variation of the algorithm used by Reichler et al., 2003). The pressure fields, p_{TP}, of the first tropopause and, if present, of the second tropopause were calculated twice a day (00:00 and 12:00 UT) from 1979 to 2010, on a horizontal grid of 1.5° lat. × 1.5° long. The tropopause heights were calculated by interpolation of the

ACPD
14, 1349–1374, 2014

geopotential heights of the two isobaric levels just above and below the tropopause pressure. A linear interpolation on the logarithm of pressure was used.

The ratio between the number of times a second tropopause is found at a given grid point and the number of times the first tropopause is calculated, in the same grid point, gives the relative frequency of DT events. Figure 1 shows the frequency of DTs in the subtropics and midlatitudes of the Northern Hemisphere for the Januaries from 1979 to 2010.

2.2 Backward trajectories

The DT events have maximum frequency of occurrence in the latitude band of 30–40° N. To study the origin of the air that ends up between DTs, 10 day back-trajectories were calculated for the 20 domains shown in Fig. 1. Eight domains were placed northward of the maxima of DT occurrence, six domains were placed along the maxima, and the remaining six domains were placed southward of the maxima of DT occurrence. The domains' placement was chosen to sample regions with different frequencies of occurrence of DTs. Backward trajectories were calculated using the 8.2 version of FLEXPART (Stohl et al., 2005), a Lagrangian Particle Dispersion Model developed at the Norwegian Institute for Air Research in the Department of Atmospheric and Climate Research, freely available at http://transport.nilu.no/flexpart.

The domains D1–D20 are boxes with horizontal dimension of 1.5° lat. × 1.5° long., centered at grid points where the STs and DTs were calculated (see Sect. 2.1). To ensure that for most cases of DT events, all particles were released between the two tropopauses, the domains' vertical boundaries (Z_1 and Z_2) were defined for each January, using the following criteria:

$$Z_1 = \overline{Z}_{\mathrm{TP1}} + 2\sigma_{\mathrm{TP1}} \quad (1)$$

$$Z_2 = \overline{Z}_{\mathrm{TP2}} - \sigma_{\mathrm{TP2}} \quad (2)$$

ACPD
14, 1349–1374, 2014

Double tropopauses formation

A. C. Parracho et al.

where $\overline{Z}_{TP1}$ and $\overline{Z}_{TP2}$ are the monthly mean heights of the first and second tropopause, respectively, with the heights standard deviations in the month represented by σ_{TP1} and σ_{TP2}. The means were calculated only for DTs events. As it may be seen in Figs. 1 and 3 of Pan et al. (2009), a layer of extratropical stratospheric air remains just above the first tropopause, when an intrusion of tropical tropospheric air occurs. Because our simulations aim to test if the tropospheric intrusions are a main mechanism for the occurrence of DTs, to better identify the intruded tropospheric air alone, we defined the lower boundary 2σ above the mean height of the first tropopause. Using the above conditions, some cases with large standard deviations may lead to domains whose thickness is smaller than 2 km. For these cases we removed a few points most distant from the mean first tropopause and recomputed the standard deviation. Using this condition in the definitions Eqs. (1) and (2), the average thickness of the domains (boxes) is about 3.5 km. The heights of the lower and upper boundary of each domain remained constant for all simulations in each January, and changed only from year to year to account for the variability in mean atmospheric circulation.

FLEXPART was run off-line, forced by the ERA Interim reanalysis fields available at 6 h intervals (00:00 UT, 06:00 UT, 12:00 UT and 18:00 UT). In order to have forcing fields at 3 h intervals, the reanalysis were complemented by the fields from 3 h and 9 h forecasts at 03:00 UT, 09:00 UT, 15:00 UT and 21:00 UT. The forcing fields are available on a grid of 1° lat. × 1° long. in the 60 levels of the reanalysis model. Ten-day back trajectories were initialized twice a day, for every month of January, between 1980 and 2010. For each run, 2000 particles were released in each domain during 6 h time intervals centered around 00:00 and 12:00 UT.

The subroutine *calcpar.f* in FLEXPART calculates the tropopause height. However, the algorithm used to compute the tropopause in the downloaded version of FLEXPART does not implement the WMO criterion (a) for the definition of the tropopause completely. The downloaded version of *calcpar.f* tests the lapse rate criterion between two levels which are 2 km apart but it does not verify if the average lapse rate does not exceed $2\,\mathrm{K\,km^{-1}}$ for all levels inside the 2 km layer. Birner (2010b) showed that the

ACPD
14, 1349–1374, 2014

tropopause level in the subtropics is very sensitive to the different ways the thickness criterion is implemented. Because DTs frequently occur in the subtropics, we changed *calcpar.f* in order to implement the thickness criterion described in Sect. 2.1, i.e. the new version of subroutine *calcpar.f* verifies if the average lapse rate does not exceed $2\,\mathrm{K\,km^{-1}}$ for all levels inside the 2 km layer.

2.3 Analysis method

Output variables from FLEXPART runs were recorded at 3 h intervals. Here, we analyse the plume centroid position coordinates (horizontal position of the center of mass of the particles released in each domain, hereafter the centroid trajectory), the mean of the potential vorticity estimated from the reanalysis fields at the position of each particle at each recorded time, and the fraction of tropospheric particles (the fraction of particles found below the tropopause).

The statistics of these variables were analysed separately for the cases of DT and ST events which were defined using the first and second tropopause heights computed from ERA Interim data, described in Sect. 2.1. Consider a domain Di centered in the point (i,j) of the 1.5° lat. × 1.5° long. grid used to construct the DT dataset. Single tropopause events, for a domain Di, were determined using the following conditions:

1. The thermal profiles at the central point (i,j) and at the grid points $(i-1,j)$, $(i,j-1)$, $(i+1,j)$ and $(i,j+1)$ have single thermal tropopauses, at the central instant t (00:00 or 12:00 UT) of the interval for the release of the particles.

2. Let $h_{5\mathrm{ST}}(t,n)$ be the mean height of the single tropopauses in the five points, at the instant t of the nth year, and let $\overline{h}_{5\mathrm{ST}}(n)$ and $\sigma_{5\mathrm{hST}}(n)$ be the monthly mean and standard deviation of $h_{5\mathrm{ST}}(t,n)$ at the nth year. Instant t is retained as a ST event, for domain Di, if the following condition is met:

$$\overline{h}_{5\mathrm{ST}}(n)-2\sigma_{5\mathrm{hST}}(n)\le h_{5\mathrm{ST}}(t,n)\le h_1(n,\ \mathrm{Di}), \tag{3}$$

where $h_1(n,\ \mathrm{Di})$ is the lower boundary of Di at the nth year.

ACPD
14, 1349–1374, 2014

Double tropopauses formation

A. C. Parracho et al.

The upper bound in Eq. (3) ensures that only the cases where the tropopause height is below the lower boundary of Di were retained in the analysis. The lower bound $\overline{h}_{5ST}(n) - 2\sigma_{5hST}(n)$ excludes events that may be due to an erroneous identification of the tropopause.

Double Tropopause events must verify the following conditions:

1. The thermal profiles at the central point (i, j) and at grid points $(i-1, j)$, $(i, j-1)$, $(i+1, j)$ and $(i, j+1)$ have multiple thermal tropopauses, at the central instant t (00:00 or 12:00 UT) of the interval for the release of the particles.

2. Let $h_{5DT1}(t,n)$ and $h_{5DT2}(t,n)$ be the mean heights of the first and second tropopauses in the five points, at the instant t of the nth year, and let $\overline{h}_{5DT1}(n)$, $\overline{h}_{5DT2}(n)$, $\sigma_{5hDT1}(n)$ and $\sigma_{5hDT2}(n)$ be the monthly means and standard deviations of $h_{5DT1}(t,n)$ and $h_{5DT2}(t,n)$, respectively, at the nth year. Instant t is retained as a DT event, for domain Di, if the following conditions are met:

$$\overline{h}_{5DT1}(n) - 2\sigma_{5hDT1}(n) \leq h_{5DT1}(t,n) \leq h_1(n, \mathrm{Di}) \tag{4}$$

$$\overline{h}_{5DT2}(n) + 2\sigma_{5hDT2}(n) \geq h_{5DT2}(t,n) \geq h_2(n, \mathrm{Di}). \tag{5}$$

where $h_2(n, \mathrm{Di})$ is the upper boundary of Di at the nth year.

Conditions (4) and (5) ensure that only cases in which the domain Di is between the two tropopauses were retained in the analysis. Although these conditions are very stringent, a total of 11 970 ST events and 4897 DT events were retained. With less restrictive conditions, using only the central point of the domains, a larger number of events would be retained. Those less restrictive conditions were tested and the results did not change qualitatively but the differences between ST and DT statistics were somewhat smaller. Because we aim to test the importance of tropospheric intrusions for the occurrence of DTs, and because tropospheric intrusions should manifest in a region larger than the horizontal extension of the domains, we decided to use the

ACPD
14, 1349–1374, 2014

above conditions. Moreover, those conditions help to avoid false identification of ST and DTs cases, which may occur using only one vertical profile, due to the vertical resolution of the reanalyses.

Before beginning the analysis of the simulations, it is useful to review the concept behind the methodology used. If the tropospheric intrusions into the lower midlatitude stratosphere are an important mechanism for the occurrence of DTs, then significant fractions of tropospheric air must reach the domains in the case of DT events. To ensure that, in the absence of tropospheric intrusions, the tropospheric air must be only found below the domains, we adopted the stringent condition that the mean height of the first tropopauses, in the central point of the domain and in the four neighboring points, is smaller than the height of the domain's bottom boundary (conditions 3 and 4). To ensure that, in the presence of tropospheric intrusions, the stratospheric air above the second tropopause does not reach the domains, we used condition 5.

The domains were fixed in space for each January, and only ST and DT events with the first tropopause (or the single for STs) below the domains were retained in the analysis. If the tropospheric intrusions are not an important mechanism for the occurrence of DTs, the air above the first tropopause, in DT cases, or above the single tropopause, in ST cases, must predominantly show similar stratospheric characteristics. On the other hand, if tropospheric intrusions are an important mechanism for the occurrence of DTs, the air above the first tropopause, in DT cases, and the air above the single tropopauses, in ST cases, must show different characteristics:, i.e. particles that reach the domains, in ST cases, must have stratospheric characteristics, and the particles that reach the domains, in DT cases, must show tropospheric characteristics.

In the following analysis we compare the characteristics of the air that reaches the domains in the cases of ST and DT events.

ACPD
14, 1349–1374, 2014

Double tropopauses formation

A. C. Parracho et al.

3 Results

3.1 Trajectory densities

In order to assess the spatial distributions of trajectories for ST and DT events, small $1^{\circ} \times 1^{\circ}$ bins were defined, covering the entire Northern Hemisphere. The number of times a (segment of a) centroid trajectory fell on each bin was counted separately for DT and ST events. Then, the number of times a bin was crossed by the centroid trajectory was divided by the total number of ST or DT events (which varied with each domain), allowing for empirical estimates of the spatial probability density functions of trajectories for both ST and DT cases. Figure 2 shows the difference fields between trajectory densities for DT and ST events for nine domains (3 located northward of the maxima of DT occurrence, 3 placed along the maxima, and 3 located southward of the maxima of DT occurrence). The results for the other domains are similar and the differences are shown for 5 day back-trajectories. Because the position of the trajectories was recorded at 3 h intervals, 40 instants were recorded for each ST or DT event. Therefore, the ratio between the number of times a bin was crossed by center of mass of the plume trajectory and the total number of ST or DT events gives a density normalized to 40. The horizontal projections of the centroid trajectories, for all domains illustrated in Fig. 2 (and also for the domains not represented), show that the air found between double tropopauses comes, on average, from lower latitudes than the air found for single tropopause cases. Although it is not shown, the density differences (DT – ST) have the same magnitude as the densities for the separate DT and ST events.

Figure 3 shows the tropopause height distributions for central points of the three domains over the North America (domains D3, D10 and D16). The bimodality of the height distribution of the single tropopause is evident. Single tropopauses with the height around the mean height of the extratropical tropopause are more common northward of the maximum occurrence of DTs; and single tropopauses with the height around the

ACPD
14, 1349–1374, 2014

mean height of the tropical tropopause are more common southward of the maximum occurrence of DTs.

Results in Figs. 2 and 3 support the hypothesis that double tropopause structures result from excursions of the tropical tropopause over the extratropical tropopause (Randel et al., 2007b; Pan et al., 2009). However, we may observe in Fig. 1 that there are regions where the frequency of DTs is over 50 %. For those regions, the DT structure has a semipermanent character, and other processes (than the excursions of the tropical tropopause) should play an important role in their development, as proposed by Birner (2010a).

3.2 PV along the trajectories

The transition between the tropical tropopause and the extratropical tropopause varies in space and time. However, the analysis of the spatial distributions of trajectories for ST and DT events does not take into consideration this variability. A dynamical field that is sensitive to the transition between the troposphere and stratosphere, and between tropical and extratropical stratosphere is the potential vorticity. The analysis of the PV field helps to characterize the dynamical region from whence the air masses found between DTs come. To begin this analysis we must examine the climatological structure of the PV field, and in particular its characteristics near the tropopause. In order to preserve PV features coupled to the tropopause, we computed the climatology by averaging the fields with respect to the local, time-dependent altitude of the first tropopause (Birner, 2006). To do that we proceeded as follows: consider a fixed horizontal grid point and let $PV(t,z)$ be the potential vorticity at height z with respect to sea level, and $Z_{\mathrm{TP1}}(t)$ be the height of the first tropopause at the same instant t. Then the time-average of PV in the tropopause based height is given by $\overline{\mathrm{PV}(t,z-Z_{\mathrm{TP1}}(t))}$, where the over line represents the time mean. Once the latter has been calculated, the vertical coordinate is readjusted using the time-averaged altitude of the tropopause,

ACPD
14, 1349–1374, 2014

$\overline{Z}_{\mathrm{TP1}}$, as:

$$\overline{z} = z - Z_{\mathrm{TP1}} + \overline{Z}_{\mathrm{TP1}}. \qquad (6)$$

Figure 4 shows the January climatology of the zonal-mean PV using the conventional vertical coordinates and the tropopause-based vertical coordinates. The PV climatology calculated using the tropopause-based height shows a strong PV gradient around the tropopause, with the isolines from 2 to 6 PVU (potential vorticity units) very close together. Above this region there is a minimum in the vertical gradient of PV. These features are not observed when the averaging is done with fixed altitude above the sea level.

The traditional meteorological approximation of PV is $P = (f + \zeta_\theta)(-g\partial\theta/\partial p)$, where g is the earth's gravity, f is the Coriolis parameter, θ is the potential temperature, and ζ_θ is the relative vorticity evaluated on isentropic surfaces (Hoskins et al., 1985). Because the static stability enters in the definition of PV through the factor $(-g\partial\theta/\partial p)$, the above characteristics of the PV field near the tropopause could be expected to be associated with the TIL. It is also emphasized that the isolines from 2 to 5 PVU are all very close to the extratropical tropopause, which may help to understand why different PV values for the definition of the dynamical tropopause appear in the literature.

In order to characterize the origin of the air masses found between DTs, we averaged the potential vorticity along the trajectories of all particles released in each ST or DT event, i.e. for each backward trajectory simulation we calculated the mean PV considering the positions of all particles (2000) at all 3 h time intervals (80), obtaining one mean PV value for each ST and each DT event. Then we calculated the distributions of the mean PV separately for ST and DT events. The results are qualitatively similar for all domains, and, in Fig. 5 we show the PV distributions considering all domains Di collectively. The solid curves represent PDFs estimated using the Kernel method (Silverman, 1986), with a normalized Kernel function. The density was evaluated in 100 equally spaced points that cover the range of values in each data set. Using the

Kolmogorov–Smirnov test (K–S test) (Wilks, 2006) the DT and ST distributions were found to be statistically different at a significance level above 99 %.

Looking at Fig. 5, it may be observed that the air particles in DT cases come from an environment of lower PV than in the ST cases. The PV distribution for the ST cases peaks at just above 7 PVU, and 81 % of ST cases have mean PV values greater than 6 PVU, which are typical in the extratropical lower stratosphere. On the other hand, the PV distribution for the DT cases peaks at a value smaller than 5 PVU, and 56 % of DT cases have mean PV values smaller than 5 PVU, which are typical in the tropopause region or in the upper tropical/subtropical troposphere. These observations agree with the idea that a significant fraction of double tropopause events could result from excursions of the tropical tropopause and tropical air over the extratropical tropopause (Randel et al., 2007b; Pan et al., 2009).

Figure 5 shows the distribution of the mean PV of the reanalysis interpolated along the trajectories, for all instants and all particles of each simulation. To analyse the time evolution of PV along the trajectories, we calculated the trajectories densities as in Sect. 3.1 but in the longitude-PV space, which was divided into 3° longitude by 0.2 PVU bins (Fig. 6). Because of the relatively short period of the backward integrations, the diabatic effects are smaller and the PV along the trajectories must remain approximately constant. This is seen as a layered structure of density distribution of PV, with ST events having higher PV values than DT events, along the entire trajectories. Figure 6 confirms that, most frequently, the particles in DT cases come from an environment having lower PV than in ST cases.

3.3 Fraction of tropospheric particles

Another useful diagnostic for the origin of the air masses found between DTs is the fraction of tropospheric particles, TPf. At each instant, FLEXPART calculates the position of each particle with respect to the local tropopause, and gives the fraction, TPf, of particles below the tropopause. For each DT or ST event we averaged the fraction of tropospheric particles along the centroid trajectory. In this averaging we excluded the

ACPD
14, 1349–1374, 2014

backward trajectory instants for which the nearest grid point to the centroid trajectory has a DT. With this approach, the ambiguity to consider a particle above or below the tropopause is avoided.

Taking the ST and DT cases separately, we calculated the box plot distributions of the fraction of tropospheric particles for each domain. As for the PV, the distributions of TPf are qualitatively similar for every domain. Therefore Fig. 7 shows the box plots of TPf considering all domains collectively. It is evident that the composition of the air masses found between DTs has much more tropospheric air than the air masses found in the same space in the ST cases. For near a quarter of DT cases the fraction of tropospheric air found between DTs is more than one half, whereas only for 2 % of ST cases is the fraction of tropospheric air more than one half. These results agree with the works of Pan et al. (2009) and Vogel et al. (2011) which analysed the occurrence of double tropopauses in association with intrusion of tropical tropospheric air into the lower extratropical stratosphere.

4 Concluding remarks

The double tropopauses (DTs) are a common feature in the subtropics and midlatitudes, mostly during the winter. The mechanisms behind the thermal structure of DTs are not completely understood. Birner (2010a) argued that DTs may be forced locally by the adiabatic heating associated with the meridional residual circulation. Randel et al. (2007b) and Pan et al. (2009) suggested that double tropopause structures could result from excursions of the tropical tropopause over the extratropical tropopause, accompanied by intrusions of tropical tropospheric air into the lower extratropical stratosphere. However, Wang and Polvani (2011) and Añel et al. (2012) argued that the air particles found between double tropopauses come from high latitudes, not from the tropics/subtropics.

Even if, for some regions, DT structures have a semipermanent character which cannot be explained by the excursions of the tropical tropopause alone, this mechanism

ACPD
14, 1349–1374, 2014

should be important for the occurrence of DTs, as suggested recently by Castanheira and Gimeno (2011); Castanheira et al. (2012) and Peevey et al. (2012). To solve the apparent contradiction with the results of Wang and Polvani (2011) and Añel et al. (2012), we performed a systematic analysis of the origin of the air found between DTs using the Lagrangian model FLEXPART. The analysis was done for every January, from 1980 to 2010. Our results show that the air masses found between double tropopauses come from regions which are equatorward (smaller latitudes) of the regions where the air masses associated with STs are found to come from. The analysis of the PV reveals that, in DT cases, the air masses come from a PV environment typical of the tropopause region and the upper tropical/subtropical troposphere, whereas, in ST cases, the air masses come mostly from a PV environment typical of the lower extratropical stratosphere. Moreover, in a large percentage of events, the air masses found between the DTs are composed in more than one half by air particles that come from the troposphere. In the case of STs, in more than 98 % of events the air masses are predominantly composed by air particles that come from the stratosphere.

In summary, the results presented in this work clearly show that processes involving excursions of the tropical tropopause over the extratropical tropopause, accompanied by intrusions of the tropical tropospheric air into the lower extratropical stratosphere, make a significant contribution to the occurrence of DTs in the subtropics and midlatitudes.

Acknowledgements. This work was partially supported by the DYNOZONE project (PTDC/CTE-ATM/105507/2008) funded by the FCT (Fundação para a Ciência e a Tecnologia, Portugal). C. A. F. Marques was supported by the FCT under grant SFRH/BPD/76232/2011.

References

Añel, J. A., Antuña, J. C., de la Torre, L., Castanheira, J. M., and Gimeno, L.: Climatological features of global multiple tropopause events, J. Geophys. Res., 113, D00B08, doi:10.1029/2007JD009697, 2008. 1351

ACPD
14, 1349–1374, 2014

Añel, J. A., de la Torre, L., and Gimeno, L.:. On the origin of the air between multiple tropopauses at midlatitudes, The Scientific World Journal, 2012, 191028, doi:10.1100/2012/191028, 2012. 1351, 1362, 1363

Birner, T.: Fine-scale structure of the extratropical tropopause region, J. Geophys. Res., 111, D04104, doi:10.1029/2005JD006301, 2006. 1351, 1359

Birner, T.: Residual circulation and tropopause structure, J. Atmos. Sci., 67, 2582–2600, doi:10.1175/2010JAS3287.1, 2010a. 1351, 1359, 1362

Birner, T.: Recent widening of the tropical belt from global tropopause statistics: sensitivities, J. Geophys. Res., 115, D23109, doi:10.1029/2010JD014664, 2010b. 1352, 1354

Birner, T., Dörnbrack, A., and Schumann, U.: How sharp is the tropopause at midlatitudes?, Geophys. Res. Lett., 29, 45-1–45-4, doi:10.1029/2002GL015142, 2002. 1351

Castanheira, J. M., and Gimeno, L.: Association of double tropopause events with baroclinic waves, J. Geophys. Res., 116, D19113, doi:10.1029/2011JD016163, 2011. 1351, 1363

Castanheira, J. M., Peevey, T. R., Marques, C. A. F., and Olsen, M. A.: Relationships between Brewer-Dobson circulation, double tropopauses, ozone and stratospheric water vapour, Atmos. Chem. Phys., 12, 10195–10208, doi:10.5194/acp-12-10195-2012, 2012. 1351, 1363

Dee, D. P., Uppala, S. M., Simmons, A. J., Berrisford, P., Poli, P., Kobayashi, S., Andrae, U., Balmaseda, M. A., Balsamo, G., Bauer, P., Bechtold, P., Beljaars, A. C. M., van de Berg, L., Bidlot, J., Bormann, N., Delsol, C., Dragani, R., Fuentes, M., Geer, A. J., Haimberger, L., Healy, S. B., Hersbach, H., Hólm, E. V., Isaksen, L., Kållberg, P., Köhler, M., Matricardi, M., McNally, A. P., Monge-Sanz, B. M., Morcrette, J.-J., Park, B.-K., Peubey, C., de Rosnay, P., Tavolato, C., Thépaut, J.-N., and Vitart, F.: The ERA-Interim reanalysis: configuration and performance of the data assimilation system, Q. J. Roy. Meteor. Soc., 137, 553–597, doi:10.1002/qj.828, 2011. 1352

Fueglistaler, S., Dessler, A. E., Dunkerton, T. J., Folkins, I., Fu, Q., and Mote, P. W.: Tropical tropopause layer, Rev. Geophys., 47, RG1004, doi:10.1029/2008RG000267, 2009. 1350

Gettelman, A., Hoor, P., Pan, L. L., Randel, W. J., Hegglin, M. I., and Birner, T.: The extratropical upper troposphere and lower stratosphere, Rev. Geophys., 49, RG3003, doi:10.1029/2011RG000355, 2011. 1350

Hoskins, B. J., McIntyre, M. E., and Robertson, A. W.: On the use and significance of isentropic potential vorticity maps, Q. J. Roy. Meteor. Soc., 111, 877–946, 1985. 1360

ACPD
14, 1349–1374, 2014

Title Page
Abstract | Introduction
Conclusions | References
Tables | Figures
◀| |▶
◀ ▶
Back | Close
Full Screen / Esc
Printer-friendly Version
Interactive Discussion

Kunz, A., Konopka, P., Müller, R., Pan, L. L., Schiller, C., and Rohrer, F.: High static stability in the mixing layer above the extratropical tropopause, J. Geophys. Res., 114, D16305, doi:10.1029/2009JD011840, 2009. 1351

Pan, L. L., Randel, W. J., Gille, J. C., Hall, W. D., Nardi, B., Massie, S., Yudin, V., Khosravi, R., Konopka, P., and Tarasick, D.: Tropospheric intrusions associated with the secondary tropopause, J. Geophys. Res., 114, D10302, doi:10.1029/2008JD011374, 2009. 1351, 1354, 1359, 1361, 1362

Peevey, T. R., Gille, J. C., Randall, C. E., and Kunz, A.: Investigation of double tropopause spatial and temporal global variability utilizing high resolution dynamics limb sounder temperature observations, J. Geophys. Res., 117, D01105, doi:10.1029/2011JD016443, 2012. 1363

Randel, W. J., Wu, F., and Forster, P.: The extratropical tropopause inversion layer: global observations with GPS data, and a radiative forcing mechanism, J. Atmos. Sci., 64, 4489–4496, 2007a. 1351

Randel, W. J., Seidel, D. J., and Pan, L. L.: Observational characteristics of double tropopauses, J. Geophys. Res., 112, D07309, doi:10.1029/2006JD007904, 2007b. 1351, 1359, 1361, 1362

Reichler, T., Dameris, M., and Sausen, R.: Determining the tropopause height from gridded data, Geophys. Res. Lett., 30, 2042, doi:10.1029/2003GL018240, 2003. 1352

Silverman, B. W.: Density Estimation for Statistics and Data Analysis, Chapman and Hall, London, 175 pp., 1986. 1360

Stohl, A., Forster, C., Frank, A., Seibert, P., and Wotawa, G.: Technical note: The Lagrangian particle dispersion model FLEXPART version 6.2, Atmos. Chem. Phys., 5, 2461–2474, doi:10.5194/acp-5-2461-2005, 2005. 1353

Vogel, B., Pan, L. L., Konopka, P., Gunther, G., Muller, R., Hall, W., Campos, T., Pollack, I., Weinheimer, A., Wei, J., Atlas, E. L., and Bowman, K. P.: Transport pathways and signatures of mixing in the extratropical tropopause region derived from Lagrangian model simulations, J. Geophys. Res., 116, D05306, doi:10.1029/2010JD014876, 2011. 1362

Wang, S. and Polvani, L. M.:, Double tropopause formation in idealized baroclinic life cycles: the key role of an initial tropopause inversion layer, J. Geophys. Res., 116, D05108, doi:10.1029/2010JD015118, 2011. 1351, 1362, 1363

Wilks, D. S.: Statistical Methods In Atmospheric Sciences, Elsevier, San Diego, California, USA, 649 pp., 2006. 1361

ACPD
14, 1349–1374, 2014

World Meteorological Organization: Meteorology: A three-dimensional science, WMO Bull., 6, 134–138, 1957. 1351, 1352

ACPD
14, 1349–1374, 2014

Double tropopauses formation

A. C. Parracho et al.

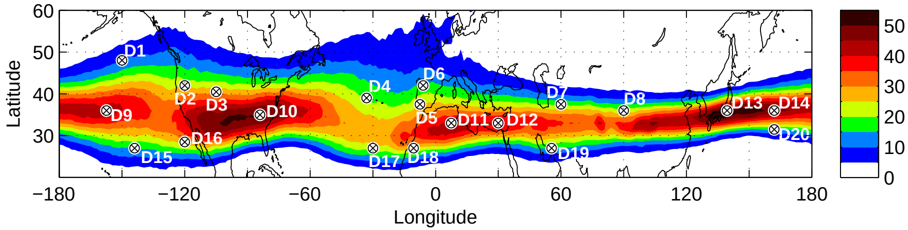

Fig. 1. Frequency of DT events for January (in %) overlaid with the twenty domains (D1–D20) used in this study.

ACPD
14, 1349–1374, 2014

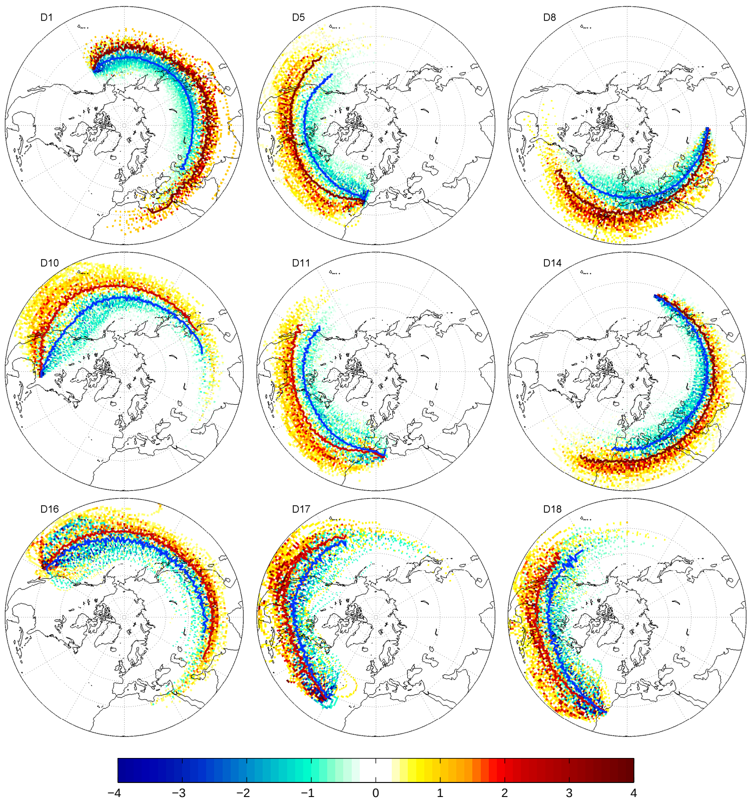

Fig. 2. Difference between DT and ST trajectory densities (DT – ST). Top to bottom rows show domains northward of the maximum occurrence of DTs, domains in the regions of maximum occurrence of DTs, and domains southward of the maximum of DTs, respectively. The differences are shown for 5 day back-trajectories. The solid lines represent the mean trajectory for ST cases (blue) and DT cases (red). The mean trajectories were calculated for bins crossed, at least, by 10 % of events.

ACPD
14, 1349–1374, 2014

Double tropopauses formation

A. C. Parracho et al.

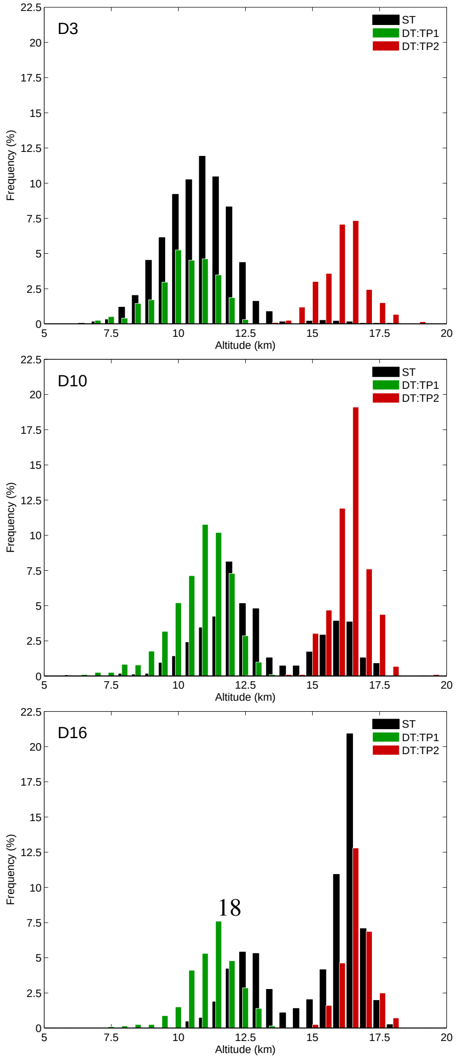

18

ACPD
14, 1349–1374, 2014

Double tropopauses formation

A. C. Parracho et al.

Fig. 3. Tropopause height distributions for ST cases (black bars) and DT cases (green bars for the first tropopause and red bars for the second tropopause). The sum of the black bars and the green bars (or red bars) gives the total frequency of 100 %. The total frequencies of first tropopauses and second tropopauses is obviously equal.

ACPD
14, 1349–1374, 2014

Double tropopauses formation

A. C. Parracho et al.

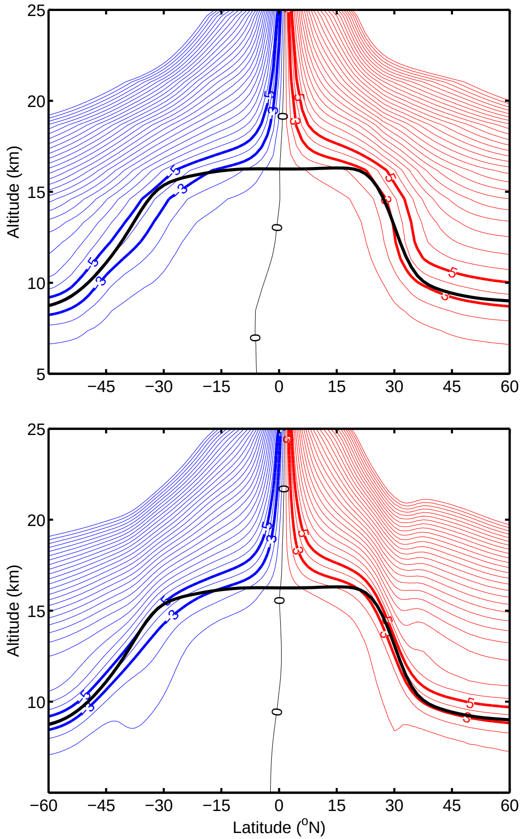

Fig. 4. January-mean, zonal-mean potential vorticity in (top) conventional vertical coordinates and in (bottom) tropopause-relative vertical coordinates. Contours were drawn at 1 PVU intervals, from 1 to 15 PVU in the NH, and −15 to −1 in the SH. The thick solid black line is the January-mean, zonal-mean height of the first tropopause. The altitude was calculated from the isobaric coordinates using $Z = 7 \times \log(p/p_s)$, where $p_s = 1000$ hPa.

ACPD
14, 1349–1374, 2014

ACPD
14, 1349–1374, 2014

Double tropopauses formation

A. C. Parracho et al.

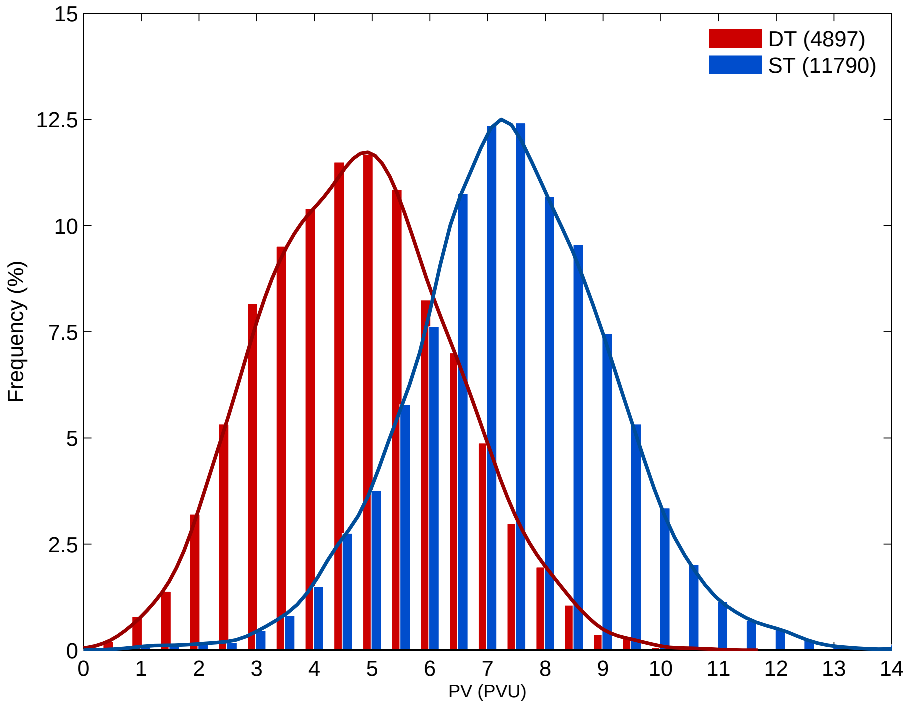

Fig. 5. Histograms and estimated PDFs of the mean potential vorticities for ST and DT events, considering all domains collectively. A total of 11 970 ST events and 4897 DT events were included in these calculations.

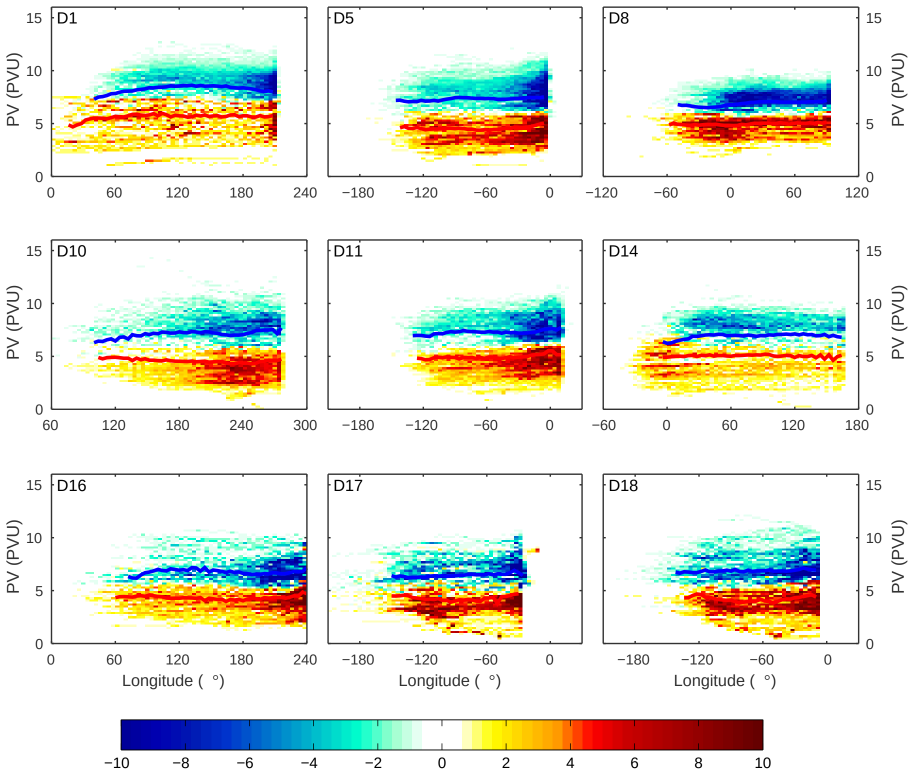

Fig. 6. Difference between DT and ST trajectory densities (DT – ST) in the longitude PV phase space, for the same domains represented in Fig. 2. The solid lines represent the mean trajectory for ST cases (blue) and DT cases (red). The mean trajectories were calculated for bins crossed, at least, by 25 % of events.

ACPD
14, 1349–1374, 2014

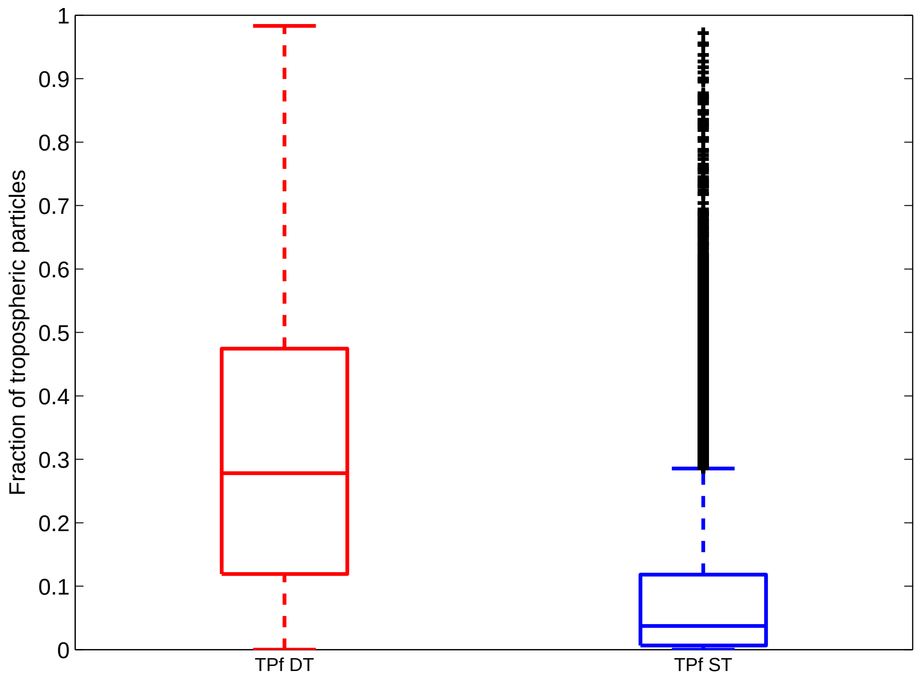

Fig. 7. Box plot diagrams of the mean fractions of tropospheric particles for ST and DT events, considering all domains collectively. Plus signs represent outliers, i.e. points at a distance from the 75th percentile that is larger than 1.5 times the difference between 25th and 75th percentile.

ACPD
14, 1349–1374, 2014

Double tropopauses formation

A. C. Parracho et al.